Bulletin of the Geological Survey of Japan, vol. 48(5), p. 257-261, 1997

Differential Laser Interferometer Apparatus for Measuring the Thermal Expansivity of Minerals at High Temperatures

Koji MASUDA*, Orson L. ANDERSON** and Dave ERSKINE***

MASUDA Koji, ANDERSON L. Orson and ERSKINE Dave (1997) Differential Laser Interferometer Apparatus for Measuring the Thermal Expansivity of Minerals at High Temperatures. *Bull. Geol. Surv. Japan*, vol. 48(5), p. 257-261, 10figs..

Abstract: In order to improve the measurement of thermal expansivity, α, at high temperatures, we have developed a new apparatus, the differential laser interferometer, to measure remotely the coefficient of thermal expansivity of minerals. Improvement on the measurement of thermal expansivity is needed since at high temperatures thermal expansivity is the least accurate of the properties needed in thermodynamic studies. Thermal expansivity data is essential in the high temperature thermal dynamics study of important minerals in the Earth. The differential laser interferometry is a new method, simultaneously monitoring two fringe signals which are 90 degree out of phase. We eliminated the error caused by heat in the signal processing. The overall sensitivity in which we can detect changes in length is about 1/100 of the wave length of the He-Ne laser (1/100 of 0.6328×10^{-6}m). We calibrated the device by measuring the thermal expansivity for single crystals of Al_2O_3 and MgO up to 1000 K.

1. Introduction

Important applications of results of high temperature elasticity are in equations of state and thermodynamics applied to geophysical problems. The coefficient of thermal expansivity, α, often appears as a multiplying factor of the several elastic constants so that the limitation of the application is controlled by the accuracy of α at high temperatures (for examples, Anderson, 1991 ; Anderson and Isaak, 1995). Values of α at temperatures higher than 1200 K are generally estimates based on extrapolation of data taken up to about 1200 K (e.g. Wachtman *et al.*, 1962 ; Suzuki *et al.*, 1979 ; Anderson *et al.*, 1992). Various experimental measurements of α often diverge at ~ 1000 K as shown in Anderson (1991). Measurements of α in the high temperature region (1500 - 1800 K) are needed. Such measurements would allow tighter constraints on thermodynamic calculations. An optical technique will provide possible requisite accuracy.

In this paper, we describe a differential laser interferometry method to measure α at high temperatures. We calibrated the device by measuring standard materials up to 1000 K.

*Environmental Geology Department, GSJ

**University of California, Los Angeles. Los Angeles, California 90095, USA.

***Lawrence Livermore National Laboratory. Livermore, California 94551, USA.

2. Differential Laser Interferometer Apparatus

2.1 Interferometer Fundamentals

Figure 1 illustrates the fundamentals of the laser interferometer. The laser beam is divided by the beam splitter and reflected on the different surfaces of the sample. The phases of the reflected beams at the beam splitter are shifted due to the difference in the path length of two beams. When two laser beams (coherent monochromatic light waves) are superimposed, the resulting intensity depends on the relative phases of the two beams. As the length D increases due to an increase in temperature, the intensity of the fringe signal at the photodiode changes. The relevant length scale of

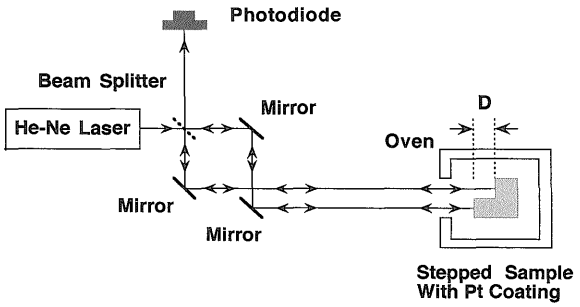

Fig. 1 Fundamentals of the laser interferometer.

Keywords: Differential Laser Interferometer, Thermal Expansivity, Al_2O_3, MgO

the fundamental laser interferometer is on the order of the wave-length of the light (0.6328×10^{-6} m for a He-Ne laser).

2.2 Differential Interferometer

The differential laser interferometer is a new interferometry method, similar to that described by Hemsing (1979) for velocity interferometers. The basic interferometer is modified to maximize sensitivity by simultaneously monitoring the two fringe signals that are 90° out of phase. These signals are obtained by adding a $\lambda/8$ retardation plate (birefringent waveplate) and a polarizing beamsplitter. Figure 2 shows the concept of the differential laser interferometer.

The $\lambda/8$ waveplate is arranged to introduce a 90° phase difference between the horizontal and the vertical polarizations of one of the divided lights traveling through the interferometer. The $\lambda/8$ waveplate induces a 45° phase lag between the horizontal and the vertical fringe phases. The light travels twice through the $\lambda/8$ waveplate; thus when recombination occurs at the beam splitter, the horizontally and vertically polarized components form two fringe patterns that are 90° out of phase. The two patterns are separated from each other by the polarizing beam splitter and then sent to two different photodiodes. Photodiode A detects the horizontal component, while B detects the vertical component of the fringe patterns.

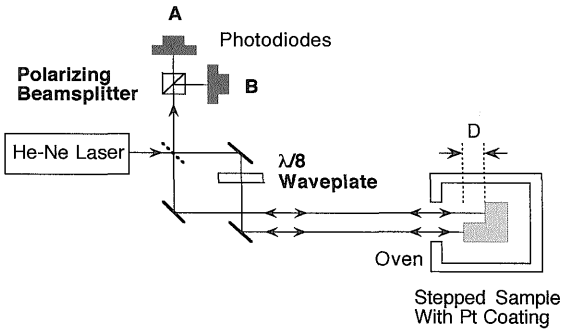

Fig. 2 Differential laser interferometer.

3. Sample

Figure 3 demonstrates the shape and dimensions of the sample used. We cut a single crystal into a cube with dimensions of 10 mm. The sample was then stepped by 5 mm so that light is reflected off two parts of the same sample, thus eliminating any possible effects due to subtle motion of the sample itself because no net path difference is introduced. The sample was coated with platinum to obtain a high reflectivity at high temperatures.

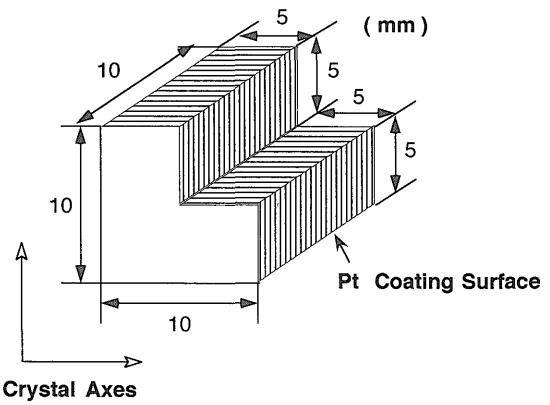

Fig. 3 Sample shape and dimensions. Shadowed areas are coated with platinum. Sample was cut along the crystal axes.

4. Data analysis

4.1 Fringe Signal Analysis

Figure 4 schematically illustrates the output of our device. A is the horizontal component and B represents the vertical component. As length, D, of the sample increases due to thermal expansion, A and B show fringe patterns (Figure 4) and are 90° out of phase. The outputs of each of the photodiodes are used as inputs for an X-Y display similar to the display of a Lissajous figure. Each fringe traces out one Lissajous figure on the scope. The passage of one fringe corresponds to D changing by $\lambda/2$, with λ being the wave length of the laser beam.

The change in angle, Ω, of the Lissajous figure can be easily measured with extreme precision. The

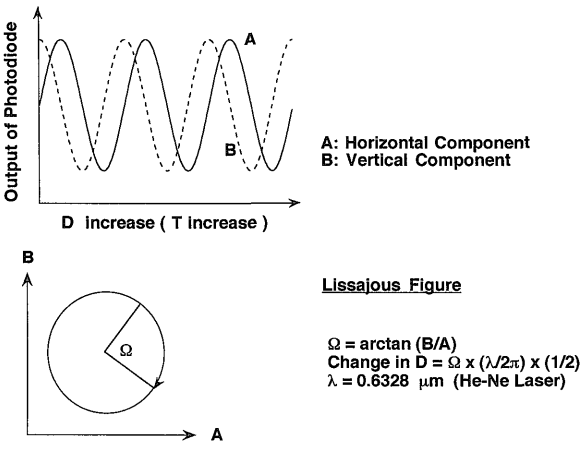

Fig. 4 Sketch of output signals and Lissajous figure. Horizontal component, A, and vertical component, B, of the fringe pattern are 90° out of phase. The trace of one Lissajous figure corresponds to a change in D of $\lambda/2$.

detection sensitivity can reach 1/100 of a wave-length. This method has been proven reliable for measuring changes in length to a fraction of a fringe of the He-Ne laser light; that is on the order of 60 Å.

4.2 Thermal Induced Path Length Correction

Care must be exercised so that the change in path length measured is due to the sample and not to the change in the distance between interferometer optics. Heating of the oven can cause the table to expand. If one interferometer arm expands more than the other, a false sample growth will appear. We performed null experiments by measuring the distance change when both laser beams reflect off the same face as the sample is heated. Any fringe shift in this arrangement is entirely due to thermally induced path length change in the distance between the optics. Figure 5 shows the observed thermal induced path length change as a function of temperature up to 1000 K. We subtract the observed thermal induced path length change from the measured data.

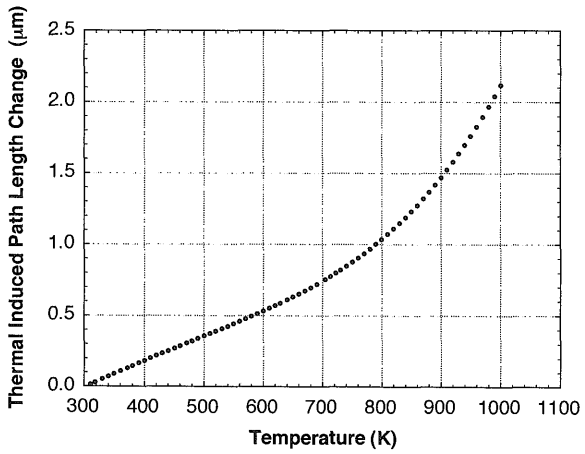

Fig. 5 Measured thermal induced path length change up to 1000 K.

4.3 Air Refraction Index

We can determine the growth of the sample step D by analyzing the phase of Lissajous, Ω,

$$\Omega = 2\pi\ (2nD/\lambda) + \text{constant}$$

Instead of measuring sample distance D, we are actually measuring $n(T)D$, where $n(T)$ is the temperature dependent refractive index of air. Increasing the temperature causes a decrease in n, which mimics a shrinking sample (of fractional change 2.045×10^{-4} at 1000 K). Thus actual sample growth values will be greater than measured. The fractional sample growth is

$$\Delta D/D_0 = \lambda\,\Delta\Omega/4\pi nD_0 - \Delta n/n$$

Figure 6 displays the fractional correction, $\Delta n/n$, as a function of temperature.

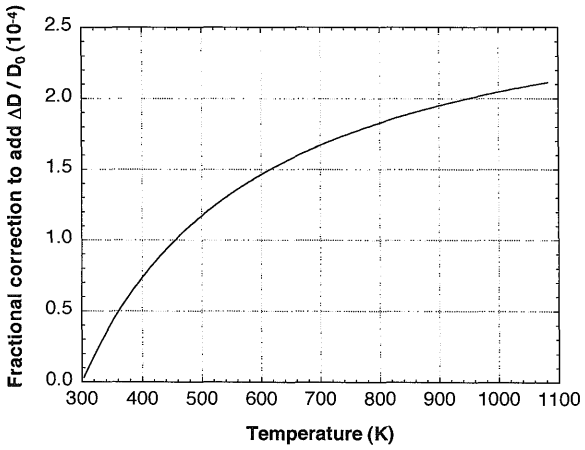

Fig. 6 Fractional correction curve to add due to the oven atmosphere index of refraction.

5. Data

We measured the thermal expansivity of single crystals of Al_2O_3 and MgO up to 1000 K in order to calibrate the differential laser interferometer. Numerous data are available on these minerals with little discrepancy between the data reported by different laboratories in the temperature range up to 1000 K.

5.1 Data on Al_2O_3

Figure 7 plots the thermal expansivity, $\Delta D/D_0$ data along the c-axis of an Al_2O_3 single crystal without any corrections. Figure 8 illustrates the thermal expansivity with corrections for thermal induced path length and air. After adjusting the thermal expansion data with the corrections described in section 4, the thermal expansivity data measured with the differential laser interferometer agrees with previous reported data by Watchman *et al.* (1962) and White and Roberts (1983) at all temperatures.

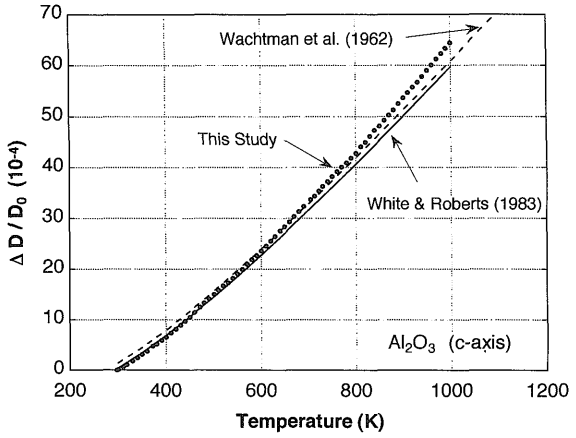

Fig. 7 Thermal expansivity of Al_2O_3 (c-axis) with no correction.

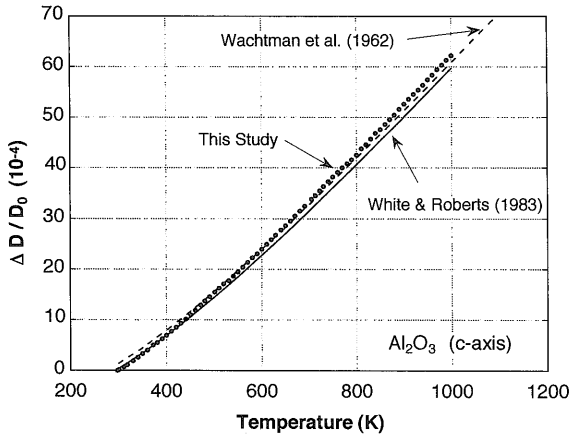

Fig. 8 Thermal expansivity of Al_2O_3 (c-axis) with corrections for thermal induced path length and air.

5.2 Data on MgO

Figure 9 sketches the thermal expansivity, $\Delta D/D_0$ data along the crystal axis of an MgO single crystal without corrections. Figure 10 shows the thermal expansivity data with thermal induced path length and air corrections. Once corrected our thermal expansivity data is close to and parallel to the data of Suzuki (1975).

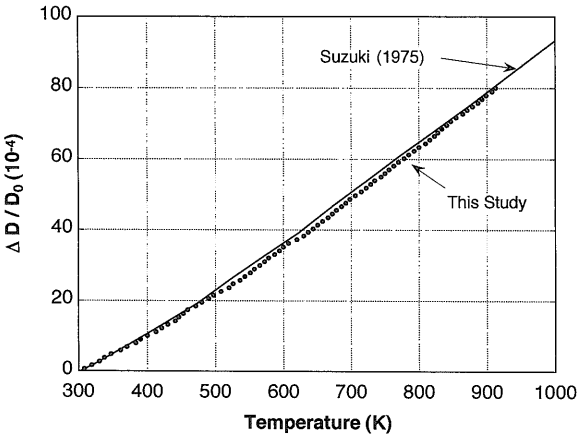

Fig. 9 Thermal expansivity of MgO with no correction.

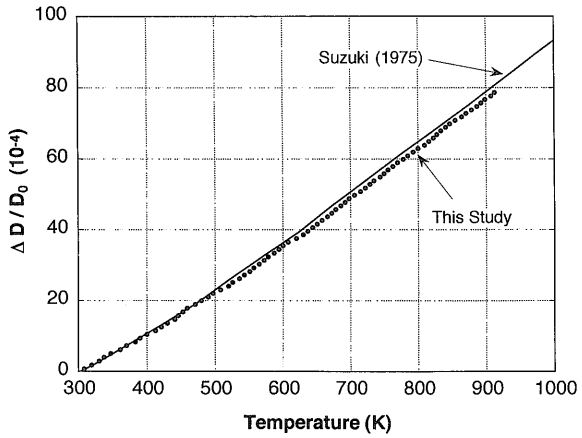

Fig. 10 Thermal expansivity of MgO with corrections for thermal induced path length and air.

6. Conclusion

We have developed a new device, the differential laser interferometer, to measure remotely the thermal expansivity of minerals. We report thermal expansivity data on Al_2O_3 and MgO crystals up to temperature of 1000 K. After adjusting for errors caused by heat, the thermal expansion data measured with the differential laser interferometer are in good agreement with reported previous data. Use of this apparatus has allowed the investigation of the high temperature thermal dynamics of important minerals, such as Mg_2SiO_4, Fe_2SiO_4, FeO, etc.

Acknowledgments: Most of this work was undertaken at the Mineral Physics Laboratory of UCLA. We thank M. Kumazawa and I. Suzuki for their encouragement throughout this work. Comments from H. Spetzler and I. Getting for the laser interferometry were very helpful. We also thank H. Tsukamoto for coating sample with Pt. MgO single crystals were provided by N. Masuda of Tateho Co. Comments from O. Nishizawa were very helpful to improve the manuscript.

References

Anderson, O. L. (1991) Accurate thermal expansivity measurements in the range 1500-2000 K are needed for minerals. *Int. J. Thermophysics,* **12**, 757-767.

Anderson, O. L. and Isaak, D. G. (1995) Elastic constants of minerals at high temperature. *In* Ahrens, J. ed., *Mineral physics and crystallography : a handbook of physical constants.* American Geophysical Union, 64-97.

Anderson, O. L., Isaak, D. G., and Oda, H. (1992) High-temperature elastic constant data on minerals relevant to geophysics. *Rev. Geophys.*, **30**, 57-90.

Hemsing, W. F. (1979) Velocity sensing interferometer (VISAR) modification. *Rev. Sci. Instrum.*, **50**, 73-78.

Wachtman, J. B. Jr., Scuderi, T. G., and Gleek, G. W. (1962) Linear thermal expansion of alumi num oxide and thorium oxide from 100° to 1100° K. *J. Amer. Ceram. Soc.*, **45**, 319-323.

White, G. K. and Roberts, R. B. (1983) Thermal expansion of reference materials: tungsten and α -Al_2O_3. *High Temperatures - High Pressures*, **15**, 321-328.

Suzuki, I. (1975) Thermal expansion of periclase and olivine, and their anharmonic properties. *J. Phys. Earth*, **23**, 145-159.

Suzuki, I., Okajima, S., and Seya, K., (1979) Thermal expansion of single-crystal manganosite. *J. Phys. Earth*, **27**, 63-69.

高温における鉱物の熱膨張係数測定のための差動型レーザー干渉計

増田幸治・Orson L. Anderson・Dave Erskine

要　旨

鉱物の熱膨張係数を非接触で測定する新しい装置，差動型レーザー干渉計，を開発・改良した．これによりこれまで精度の低い値しか得られていなかった高温下での熱膨張係数を高い精度で測定することができ，地球内部物質の熱力学的研究にとって重要なデータを提供できる．高温下での熱膨張係数は熱力学的研究に必要な係数のうち現在もっとも精度が低い値しか得られていないので，熱膨張係数測定法の改良が必要とされてきた．差動型レーザー干渉法は，90度位相のずれた2つのしま模様信号を同時にモニターする．信号処理の段階で熱によって発生する誤差を取り除いた．長さ変化の検出精度はHe-Neレーザーの波長（0.6328×10^{-6}m）の約100分の1である．Al_2O_3とMgOの単結晶の熱膨張係数を約1000Kまで測定し，装置の検定を行い，これまでに測定されたデータと比較したところ，差動型レーザー干渉計は高い精度を与えることが分かった．

（受付：1996年12月9日；受理：1997年3月7日）